Progress In Electromagnetics Research B, Vol. 53, 355–371, 2013

MIMO RADAR TRANSMIT BEAMPATTERN SYNTHESIS VIA MINIMIZING SIDELOBE LEVEL

Haisheng Xu*, Jian Wang, Jian Yuan, and Xiuming Shan

Department of Electronic Engineering, Tsinghua University, Beijing 100084, P. R. China

Abstract—In multi-input multi-output (MIMO) radar transmit beampattern synthesis, most current literature formulates the problems in steradian space. However, since the beampattern and its parameters are both measured and defined in radian space, from the view point of physical meaning, it will be better to reformulate the problems in radian space rather than in steradian space. In this paper, we propose methods in the radian space to synthesize beampatterns based on minimizing sidelobe level for the two main designs in MIMO radar, i.e., minimum sidelobe beampattern design (MSBD) and beampattern matching design (BMD). For MSBD, the design criteria considering both peak sidelobe level and integrated sidelobe level is proposed. By this we can have a good tradeoff between the intensity and power distribution in beampattern synthesis. After a two-step converting, the formulation of the criteria is transformed into a convex programming, where a global optimal solution can be obtained. For BMD, instead of minimizing mean square error directly as in conventional methods, we propose a power-approximation-based method by minimizing integrated sidelobe level. Finally, numerical comparisons with classical methods demonstrate that the proposed MSBD maintains for all range of main lobe width and the proposed BMD has smoother main lobes with maximal power focused in.

1. INTRODUCTION

Transmit beampattern synthesis is one of the most important tasks in radar system design [1–6]. In conventional phased-array radars, directionality of the transmit beam is achieved by coherently accumulating phase shifts of all the emitting elements that transmit

Received 22 June 2013, Accepted 10 August 2013, Scheduled 14 August 2013

* Corresponding author: Haisheng Xu (xhs11@mails.tsinghua.edu.cn).

the same waveform. And when the number of the array elements is large, highly focused beampatterns can be obtained. In multi-input multi-output (MIMO) radars, antennas transmit uncorrelated waveforms, which results in wide or omnidirectional beampatterns [7–11]. Sometimes it is necessary to have a trade-off between these two extremes so that a wide range of area can be illuminated and no power is wasted at the uninterested area [12]. To this end, there has been extensive work on transmit beampattern synthesis. And the work is mainly divided into two categories: one is to minimize the sidelobe level as its main objective [13, 14], and the other is to match the beampattern to a known shape [14–19]. For the former design case, [13, 14] proposed a minimum-sidelobe-based method to design the transmit beampattern in steradian space. However, since the beampattern and its parameters are both measured and defined in radian space, we shall expect that a better formulation of the beampattern synthesis is in radian space instead of steradian space. Moreover, it is not enough to reduce the sidelobe level just by maximizing the peak-intensity difference between the main lobe and the side lobes. In addition, only maximizing the intensity-difference may split the main lobe into small lobes, which gets more obvious when the desired main lobe becomes wider. And defining the sidelobe as the area outside twice the main lobe may not fully capture the sidelobe region. Finally, the method does not work when the width of the main lobe is greater than or equal to 90° because the sidelobe region cannot be defined any more. For the latter design case, most of the literature is mainly to synthesize beampatterns from the perspective of shape approximation. The existing work either uses convex optimization [14] or uses iterative algorithms [15–19] to do shape approximation by minimizing mean square error (MSE) between the designed and desired beampatterns. The main defect of these shape-approximation-based methods (SAMs) is using excessive mathematical derivations and is not very efficient, especially when using iterative algorithms. Additionally, pursuing minimum MSE by the SAMs may result in rough main lobes.

In this paper, we take a new perspective to study transmit beampattern design problems to address the above issues. In Section 2, we revisit MIMO Radar transmit beampattern and reformulate it into three spaces: spherical area-space, steradian-space and radian-space. Then in Section 3, minimum sidelobe beampattern design (MSBD) and beampattern matching design (BMD) in the radian-space are studied. For MSBD, the design criteria and its corresponding optimal solution are proposed. The method considers both peak sidelobe level and integrated sidelobe level, which can offer a good trade-off between the intensity and power distribution in beampattern synthesis. For

BMD, different from minimizing mean square error directly as in the conventional methods, we propose a power-approximation-based method by minimizing integrated sidelobe level. To verify the proposed design methods, we conduct simulations in Section 4 to show that our method for MSBD maintains for all range of main lobe width and our method for BMD can match well with the desired beampattern and have smooth main lobes with maximal power concentrated in. Finally, Section 5 concludes the paper.

Notation: we use lowercase italic letters to denote scalars, lowercase and uppercase letters in bold denote the vectors and the matrices, respectively. Superscripts T and H represent the transpose and complex conjugate-transpose (or Hermitian) operators of a matrix, respectively, while $\mathbf{tr}\{\cdot\}$ represents the trace of a square matrix. We use $\oint$ for a closed surface area integral and $\int$ for a definite integral.

2. REFORMULATION ON MIMO RADAR TRANSMIT BEAMPATTERN

Consider a MIMO radar system equipped with a uniform linear array (ULA) of M antennas vertically arranged with half-wavelength inter-sensor spacing (see Fig. 1), then the average radiation power at a differential area element dA on a sphere $S(r)$ is given by [7, 16]

$$P(r,\phi,\theta) = \frac{1}{4\pi r^2}\mathbf{a}^H(\theta)\mathbf{R}\mathbf{a}(\theta) \tag{1}$$

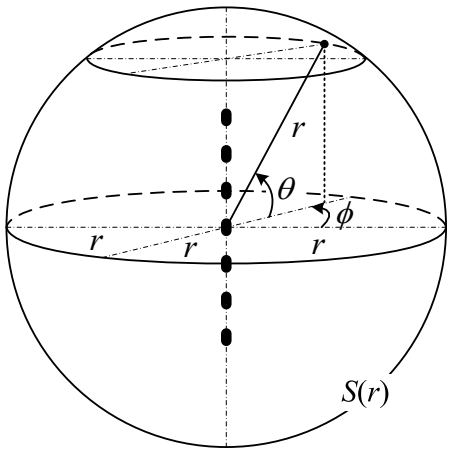

Figure 1. Spherical coordinates for MIMO radar.

where $\mathbf{R}$ is the covariance matrix of the transmitted signals, and θ ($\theta \in [-\pi/2, \pi/2]$) and ϕ ($\phi \in [-\pi, \pi]$) can be viewed as latitude and longitude of the spherical coordinates, respectively. $\mathbf{a}(\theta)$ is the steering vector of the antenna array

$$\mathbf{a}(\theta) = \left[\begin{array}{cccc} 1 & e^{j\pi \sin(\theta)} & \cdots & e^{j\pi(M-1)\sin(\theta)} \end{array} \right]^T \tag{2}$$

Integrating the spherical power density in (1) at sphere $S(r)$, we get the gain power P_G after transmit beamforming:

$$\oint_{S(r)} P(r, \phi, \theta)\, dA = P_G \tag{3}$$

Instead of normalizing the spherical power density $P(r, \phi, \theta)$ as in [7, 16], we reformulate the power density from the perspective of integral space conversion. Thus we convert the differential area element dA into steradian (Ω) space, i.e., let $d\Omega = dA/r^2$, then the power density at steradian-space can be formulated as

$$P(\phi, \theta) = \frac{1}{4\pi} \mathbf{a}^H(\theta) \mathbf{R} \mathbf{a}(\theta) \tag{4}$$

where (4) is the so-called transmit beampattern.

On the other hand, based on Fig. 1 we can easily convert the area element dA into a radian (or angular) differential, i.e., $dA = r^2 \cos(\theta) d\phi d\theta$. Then the closed surface integral in (3) can be turned into a double integral in spherical coordinates. Integrate the integrand in (3) by ϕ, then the power density in the radian-space of θ is obtained as

$$P(\theta) = \frac{1}{2} \mathbf{a}^H(\theta) \mathbf{R} \mathbf{a}(\theta) \cos(\theta) \tag{5}$$

From the above analysis, we can make the following remarks.

- Actually, we can term all the expressions of (1), (4) and (5) as *transmit beampattern* because they denote the transmit-power density of ULA MIMO Radar from three different spaces, i.e., spherical area-space, steradian-space and radian-space, respectively. The conventional transmit beampattern defined in (4) just denotes the power density at θ in steradian-space, if want to accurately characterize the power density at θ in radian-space, there should be a weighting function $\cos(\theta)$ introduced as in (5).
- In conventional MIMO transmit beampattern synthesis (beampattern matching), the main objective is to design a beampattern that approaches a desired shape. And there is no need to consider in which space the expression of beampattern should be. However, if we want to design the beampattern by minimum sidelobe level in θ-space, it is more preferable to use (5) than (4).

3. MINIMUM SIDELOBE ALGORITHM DESIGN

3.1. Minimum Sidelobe Beampattern Design

3.1.1. Design Criteria

In antenna patterns, the radiation is often characterized by three kinds of lobes, i.e., main lobe, side lobe and back lobe. See Fig. 2(a), we show a sketch map of a normalized antenna pattern. To evaluate an antenna's radiation performance, there are two important parameters, the first one is the angular width of the main lobe, i.e., beamwidth, the second one is the sidelobe level (since the designed pattern of this paper is performed in θ-space ($\theta \in [-\pi/2, \pi/2]$), the back lobes will not be considered in this paper). Beamwidth is commonly denoted by half power beamwidth (HPBW), which is the angular width of the main lobe at half-power (or -3 dB (decibels) power) points, or the first null beamwidth (FNBW), which is the angular width between the first nulls on either side of the main lobe (see Fig. 2(a)). Sidelobe level is generally denoted by the ratio (often measured in dB) of the peak value of the prominent side lobes to the peak value of the main lobe.

In [13, 14], a minimum sidelobe beampattern design method based on maximizing the peak-intensity difference between the main lobe and the side lobes is proposed. However, the method that only maximizes intensity-difference cannot sufficiently focus the power inside the

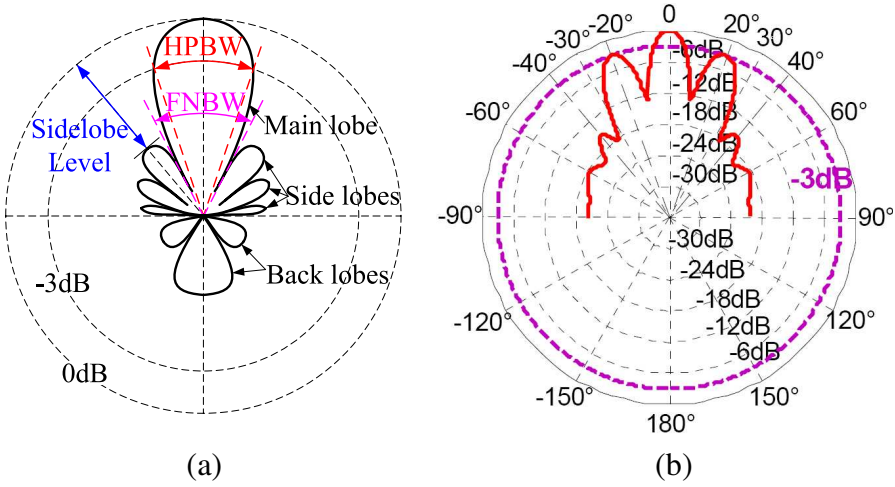

Figure 2. (a) Antenna radiation pattern; (b) beampattern with HPBW $= 40°$ designed by the method of [13, 14].

HPBW because the maximum difference may be obtained at the cost of power loss in HPBW. Besides, the method cannot be used when HPBW $\geq 90^\circ$, and the definition of sidelobe area defined by the region outside twice the HPBW is not always successful in identifying the sidelobe area because sometimes the peak intensity of the prominent side lobes may be inside the region of twice the HPBW. Fig. 2(b) shows a simulation result of the method when HPBW is 40°. From the figure, it can be seen that the region of HPBW has been spitted into three small lobes. And the positions of the peak values of the prominent side lobes outside HPBW in the figure are $\pm 39^\circ$ which are outside the defined sidelobe region $[-90^\circ, -40^\circ] \cup [40^\circ, 90^\circ]$. In addition, the method uses $P(\phi, \theta)$ to design the beampattern, as a result, the intensity at $\pm 90^\circ$ in the figure does not approach $-\infty$ as depicted in Fig. 2(a). Though the intensity at two sides approaching $-\infty$ cannot be regarded as a basis to judge the rationality of the method, the method is not rigorous. This is because the beampattern synthesis is performed in radian (θ)-space but the method based on $P(\phi, \theta)$ cannot reflect the power distribution in radian-space because $P(\phi, \theta)$ indeed characterizes the beampattern in steradian (Ω)-space.

To improve the design method, the design rule is reconsidered. First, the formulation of the transmit beampattern $P(\theta)$ in θ-space is used. Second, the range of the intensity in HPBW are considered. Third, to minimize the sidelobe level, the intensity and power (energy) of the side lobes should be considered. Therefore, besides the peak sidelobe level (PSL), we also introduce the integrated sidelobe level (ISL) as did in synthetic aperture radar (SAR) image assessment [20, 21] where ISL is used to assess how much energy of an imaged target leaks to the sidelobe region. Based on the above description, the minimum sidelobe level design criteria in transmit beampattern synthesis for MIMO radar can be stated as follows:

(a) Within HPBW, all of the radiation intensity should be higher than the half power intensity.

(b) Minimizing the PSL by minimizing the ratio of sidelobe intensity to mainlobe intensity instead of the difference.

(c) Minimizing the ISL to focus the power inside the HPBW as much as possible.

(d) When the HPBW is fixed, to reduce the power leakage outside the HPBW, narrow the FNBW as much as possible by defining the region outside HPBW all as the sidelobe region.

3.1.2. Implementation

Assume θ_0 denotes the intended direction and let $\theta_2 - \theta_1$ determine the HPBW, then based on the design criteria depicted in Section 3.1.1, we seek to find a beampattern that solves the following optimization problem:

$$\min_{\mathbf{R}} \quad \max_{t_1,t_2} \quad (t_1, t_2) \tag{6}$$

$$\text{s.t.} \quad 0.5P(\theta_0) \le P(\theta) \le P(\theta_0), \quad \forall\ \theta \in \Theta_m \tag{7}$$

$$P(\theta)/P(\theta_0) \le t_1, \quad \forall\ \theta \in \Theta_s^{'} \tag{8}$$

$$\frac{\int_{\Theta_s} P(\theta)\ d\theta}{\int_{\Theta_m} P(\theta)\ d\theta} \le t_2 \tag{9}$$

$$P(\theta_1) = 0.5P(\theta_0) \tag{10}$$

$$P(\theta_2) = 0.5P(\theta_0) \tag{11}$$

$$R_{mm} = P_G/M, \quad m = 1, 2, \ldots, M \tag{12}$$

$$\mathbf{R} \ge 0 \tag{13}$$

where (7) is defined to assure the radiation intensity inside HPBW higher than the half power intensity, (8) and (9) means minimizing the PSL and ISL, $\Theta_m = [\theta_1, \theta_2]$ is the region of HPBW and $\Theta_s = [-\pi/2, \theta_1) \bigcup (\theta_2, \pi/2]$ denotes the sidelobe region, $\Theta_s^{'}$ is just a proper subset of Θ_s and represents the region outside FNBW. Minimizing the ISL over the entire region outside the HPBW will reduce not only the sidelobe power but also the FNBW. And the reason for defining the sub-region of Θ_s as $\Theta_s^{'}$ is because the sidelobe region that needs to be reduced when minimizing the PSL is always outside FNBW and there is no need to extend $\Theta_s^{'}$ to Θ_s.

For the above optimization problem, it can be easily re-formulated by

$$\min_{\mathbf{R},t} \quad t \tag{14}$$

$$\text{s.t.} \quad 0.5P(\theta_0) \le P(\theta) \le P(\theta_0),\ \forall\ \theta \in \Theta_m \tag{15}$$

$$P(\theta)/P(\theta_0) \le t, \quad \forall\ \theta \in \Theta_s^{'} \tag{16}$$

$$\frac{\int_{\Theta_s} P(\theta)\ d\theta}{\int_{\Theta_m} P(\theta)\ d\theta} \le t \tag{17}$$

$$P(\theta_1) = 0.5P(\theta_0) \tag{18}$$

$$P(\theta_2) = 0.5P(\theta_0) \tag{19}$$

$$R_{mm} = P_G/M, \quad m = 1, 2, \ldots, M \tag{20}$$

$$\mathbf{R} \ge 0 \tag{21}$$

The above optimization problem is nonconvex since the left sides in (16) and (17) are not convex functions of $\mathbf{R}$. However, notice that if there is any $\mathbf{R}$ that can make t the least, then one of the two constraints (16) and (17) will be active and the other inactive. And we can get rid of the inactive constraint for the problem. Therefore one of the remaining work for us is to examine which one is the inactive constraint. Generally speaking, the ISL is greater than PSL in SAR image assessment where the sidelobe region is often defined as the region outside twice the HPBW. So we have reasons to suppose that the ISL is greater than PSL in our problem since the sidelobe region defined in this paper is increased and is the entire region just outside HPBW. In addition, the region Θ_s' is unknown, which makes it difficult to consider the PSL directly. Based on the aforementioned two points, we choose (17) as the active one and ignore the constraint (16) at first. Considering (17), it can be simplified and can be substituted by

$$\int_{\Theta_s} P(\theta)\ d\theta \leq \frac{t}{1+t} P_G \tag{22}$$

For $P_G = \mathbf{tr}\{\mathbf{R}\}$ while $\mathbf{R}$ can be easily normalized, therefore let $P_G = 1$ without loss of generality. Then the minimum optimization problem ((14)–(21)) can be reworked as

$$\min_{\mathbf{R},t} \quad t \tag{23}$$

$$\text{s.t.} \quad 0.5P(\theta_0) \leq P(\theta) \leq P(\theta_0),\ \forall\ \theta \in \Theta_m \tag{24}$$

$$\int_{\Theta_s} P(\theta)\ d\theta \leq \frac{t}{1+t} \tag{25}$$

$$P(\theta_1) = 0.5P(\theta_0) \tag{26}$$

$$P(\theta_2) = 0.5P(\theta_0) \tag{27}$$

$$R_{mm} = 1/M, \quad m = 1, 2, ..., M \tag{28}$$

$$\mathbf{R} \geq 0 \tag{29}$$

Now the problem of (23)–(29) becomes a convex optimization, and the optimal solution $\mathbf{R}$ can be obtained [22]. If the solution $\mathbf{R}$ also satisfies the constraint (16), then we can conclude the obtained $\mathbf{R}$ is also the optimal solution of the original problem (6)–(13).

But then again, the solved $\mathbf{R}$ at some desired HPBWs may not satisfy the constraint (16) because we obtain $\mathbf{R}$ just by (17). In this case, it means that we can not assume (16) as the inactive constraint any more, and instead, we should consider it as the active constraint. Though (16) does not satisfy the condition of a convex optimization in which the left side of a less inequality should be a convex function, it can not prevent us from finding the minimum value of t ($t_{\min}$) because

$t_{\min}$ is surely achieved at the following condition: PSL $= t_{\min}$ for (16) and ISL $\leq t_{\min}$ for (17). To obtain the $t_{\min}$, we can succeed by solving a convex optimization problem: since P_G has been equal to 1, it can be proved that the peak intensity $P(\theta_0) \leq 2/|\theta_2 - \theta_1|$ (here θ_1 and θ_2 are measured in radians), letting $t \leq kt$ where k is a constant and $k \geq 1$, then we replace (16) by a constraint containing a larger set of $(\mathbf{R}, t(\mathbf{R}))$:

$$P(\theta) \leq \frac{2kt}{|\theta_2 - \theta_1|}, \quad \theta \in \Theta_s^{'} \tag{30}$$

where k can be reckoned as a scaling factor to assure that the new feasible set is enough to contain the original set.

Calculate the FNBW of the beampattern by solving the problem of (23)–(29) to obtain $\Theta_s^{'}$, then, we substitute (30) for (16) to reformulate the problem of (14)–(21) to form a convex optimization. Setting a constant value of k then solving the optimization and comparing the calculated values of PSL with the obtained $t_{\min}$: if PSL $= t_{\min}$ then the optimal solution is obtained, otherwise, resetting k (if PSL $> t_{\min}$ then decreasing k else increasing k), then resolving the convex optimization. Repeat these operations till the condition PSL $= t_{\min}$ comes into existence.

3.2. Beampattern Matching Design

3.2.1. Main Idea

Beampattern matching is to maximize the transmitted power towards a number of regions of interest and minimize it in all other regions. See Fig. 3 for example, the interested regions are denoted by three main lobes, then beampattern matching is to synthesize a beampattern that well matches the desired shape (Generally speaking, the desired (or ideal) beampatterns are often at rectangular shapes because we always pursue that the interested area is illuminated uniformly by a radar). At present, most of the literature for BMD [14–19] is mainly to synthesize beampatterns from the perspective of shape approximation by minimizing MSE directly. The main defect of these SAMs is using excessive mathematical derivations and is not very efficient, especially when using iterative algorithms. Additionally, keeping on minimizing MSE for the SAMs may result in rough main lobes.

In the following, we will do the beampattern matching design from a different perspective: since the desired beampatterns are always to be in the hope of concentrating all power in main lobes, we can consider synthesizing beampatterns from the perspective of power approximation by minimizing the ISL, which can maximize the

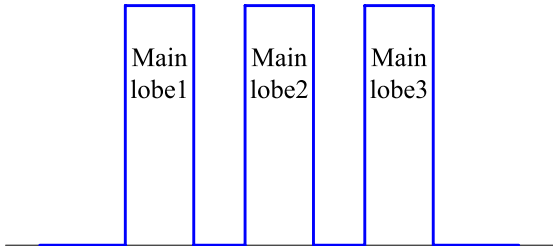

Figure 3. An idea beampattern with serval interested regions.

transmit power in main lobes (the interested area). In addition, we will still synthesize beampatterns in radian-space by $P(\theta)$ instead of in steradian-space by $P(\phi, \theta)$ for the design error we measured is in radian-space not in steradian-space. For our power-approximation-based method (PAM), it can be stated by two steps:

(a) First, find the optimal $\mathbf{R}$ which can focus the power in mainlobe region as much as possible. And we should assure that no matter how much the transmit power is, the ISL is not changed. The unchangeable ISL means that the shape of the beampattern based on the $\mathbf{R}$ will be independent of the transmit power. Therefore, this step is to complete basic shape design.

(b) Second, scaling the $\mathbf{R}$ to well match with the desired beampattern at the sense of minimum MSE. And this step is to complete the amplitude design.

3.2.2. Implementation

Based on the desired beampattern, we divide the whole radian-space Θ ($\Theta = [-\pi/2, \pi/2]$) into two parts: Θ_m and Θ_s, which are denoted as the mainlobe region and sidelobe region, respectively. To find the optimal $\mathbf{R}$ for the first step, we consider the following optimization:

$$\min_{\mathbf{R},t} \quad t \tag{31}$$

$$\text{s.t.} \quad 0.5P_0(\theta_0) \leq P_0(\theta) \leq P_0(\theta_0), \ \forall\ \theta \in \Theta_m \tag{32}$$

$$\int_{\Theta_s} P_0(\theta)\ d\theta \leq tP_G/(1+t) \tag{33}$$

$$R_{mm} = P_G/M, \quad m = 1, 2, \ldots, M \tag{34}$$

$$\mathbf{R} \geq 0 \tag{35}$$

where $P_0(\theta)$ denotes the basis of the designed beampattern in which the power in the destined mainlobe region is maximal.

Solving the above convex optimization then the optimal basis $P_0(\theta)$ is obtained. It can be seen that the shape of $P_0(\theta)$ is independent of P_G for which can be cancelled when normalizing $\mathbf{R}$. After completing the first step, introducing a scaling factor k and letting the wanted beampattern $P(\theta)$ express as $P(\theta) = kP_0(\theta)$, then minimizing the following cost function to perform the second step:

$$C(k) = \frac{1}{\pi}\int_{\Theta}(kP_0(\theta) - P_d(\theta))^2 d\theta \tag{36}$$

Obviously, the minimum value of (36) is obtained at the stationary point of $\partial C(k)/\partial k = 0$, therefore the expression of the designed beampattern is formulated by

$$P(\theta) = \frac{\int_{\Theta} P_0(\theta)P_d(\theta)d\theta}{\int_{\Theta} P_0^2(\theta)d\theta}P_0(\theta) \tag{37}$$

4. SIMULATION RESULTS

In this section, we present numerical simulations to demonstrate the effectiveness of the proposed algorithms. For the MIMO radar scenario, a ULA of $M = 10$ sensors is used for both of the minimum sidelobe Beampattern Design and beampattern matching design.

4.1. Minimum Sidelobe Beampattern Design

In the simulation, four HPBWs (denoted by B_w) with the same intended direction $\theta_0 = 0^\circ$ are considered: $B_{w1} = 30^\circ$, $B_{w2} = 80^\circ$, $B_{w3} = 90^\circ$ and $B_{w4} = 100^\circ$. The area outside $[\theta_1, \theta_2]$, where $\theta_1 = -B_w/2$ and $\theta_2 = B_w/2$, is regarded as the sidelobe region Θ_s in the whole simulation. And the measured values of HPBW, FNBW, PSL and ISL are considered as the evaluation indices.

To perform a validation on our method (denoted as M2), we implement the method proposed in [13, 14] (denoted as M1) to be compared with our approach. In the comparison, the weighting factor $\cos(\theta)$, which does not affect the method itself, is also introduced in M1 to increase the comparability. And since M1 is only valid when $B_w < 90^\circ$, therefore we only compare M1 with M2 for the cases B_{w1} and B_{w2}. Figs. 4(a) and 4(b) show the results of the two cases. From the two subfigures, it can be seen that the desired HPBW regions have been spitted into small lobes when using M1, and these small lobes consist of a newly formed main lobe and serval symmetrical side lobes. On the other hand, this phenomenon does not occur in M2 and a good performance is achieved. The calculation results presented in Table 1 further support our conclusion.

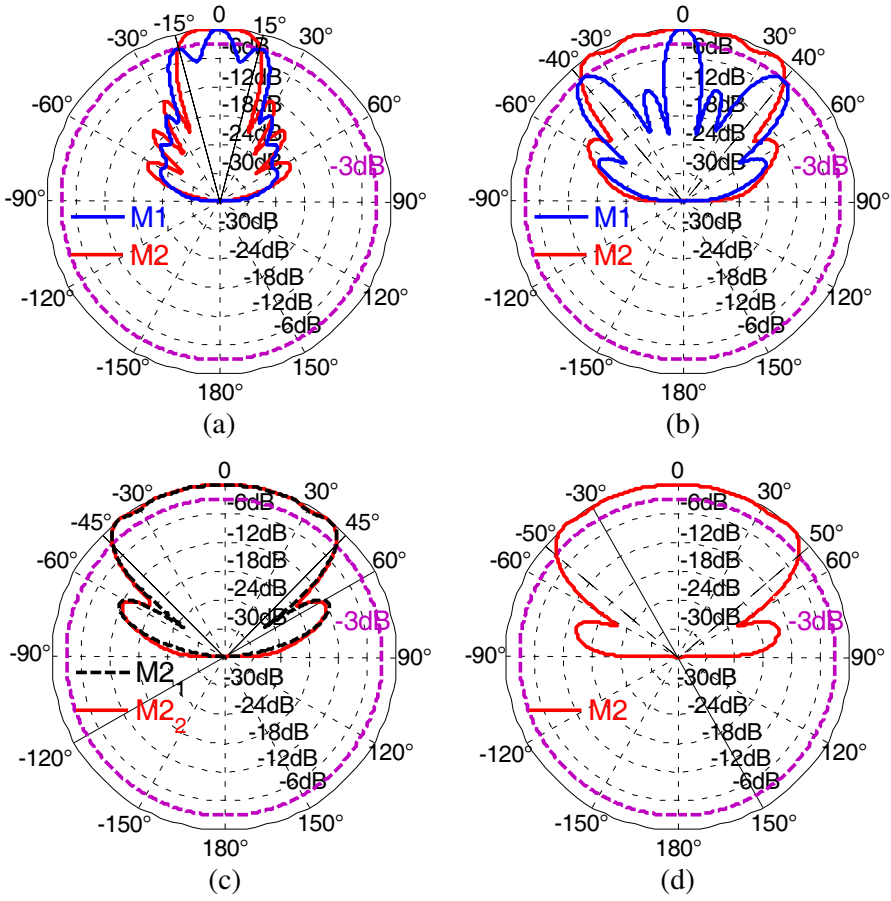

Figure 4. Minimum sidelobe beampattern design with (a) HPBW = 30°; (b) HPBW = 80°; (c) HPBW = 90°; (d) HPBW = 100°.

In addition, we also show that our method (M2) have a good performance when $B_w \geq 90°$, as shown in Figs. 4(c) and 4(d) and the corresponding entries in Table 1. It should be noted that the graphs depicted by red lines in the four sub-figures ((a)–(d)) are the final beampatterns obtained by M2. And the optimal beampatterns for the cases B_{w1}, B_{w2} and B_{w4} is directly synthesized by solving the convex optimization of (23)–(29) because the optimal solutions of the three cases all satisfy the condition that the PSL should be lower than the ISL. However, B_{w3} is not the case. That is why there are two patterns shown in Fig. 4(c): $\mathrm{M2}_1$ denotes the pattern obtained by

Table 1. Performance parameters of the design results.

B_w		HPBW	FNBW	PSL	ISL
$B_{w1} = 30°$	M1	10.08°	17.64°	−2.98 dB	−3.46 dB
	M2	30°	45.36°	−12.32 dB	−7.96 dB
$B_{w2} = 80°$	M1	10.30°	23.4°	−2.98 dB	−3.91 dB
	M2	80°	99.72°	−13.18 dB	−11.58 dB
$B_{w3} = 90°$	$M2_1$	90°	107.76°	−11.51 dB	−12.54 dB
	$M2_2$	90°	109.32°	−12.30 dB	-12.30 dB
$B_{w4} = 100°$	M2	100°	126.12°	−14.14 dB	−12.47 dB

the formulation of (23)–(29), which is not the optimal solution of the original problem because the PSL is higher than the ISL (see Table 1); while $M2_2$ denotes the optimal solution and is obtained by using the following steps: firstly, based on the calculated FNBW by (23)–(29), we fix the specific region of Θ'_s, then reformulate the optimization of (14)–(21) by substituting (30) for (16) to resolve the optimal solution as having been mentioned in Section 3.1.2. In $M2_2$, we fix $\Theta'_s = [-90°, -53.88°] \bigcup [53.88°, 90°]$ by the calculated FNBW = 107.76°. And the optimal solution is obtained at $t_{\min} = \text{PSL} = \text{ISL} = -12.30\,\text{dB}$ when $k = 1.1297$.

4.2. Beampattern Matching Design

In this simulation, we consider four desired beampatterns: one interested area with a beamwidth of 22° for case 1 and a wider beamwidth of 60° for case 2, and two and three interested areas with each beamwidth of 30° for case 3 and case 4, respectively. The dash lines in Figs. 5(a)–5(d) have shown the four desired beampatterns, respectively. To further validate our method, we compare it with the SAM proposed in [14] for which can obtain the optimal beampattern form the perspective of shape approximation by minimizing MSE. In the comparison, besides comparing the beampatterns of the two methods with the desired one in shape evaluation, MSE and ISL are also calculated as numerical evaluations.

Observing the four subfigures (Figs. 5(a)–5(d)), it can be seen that the beampatterns obtained by our method (denoted as PAM) and the SAM both have good shapes to match with the desired ones. And the differences between PAM and SAM are that the former (our method) has lower sidelobe level and smoother main lobes. Calculating

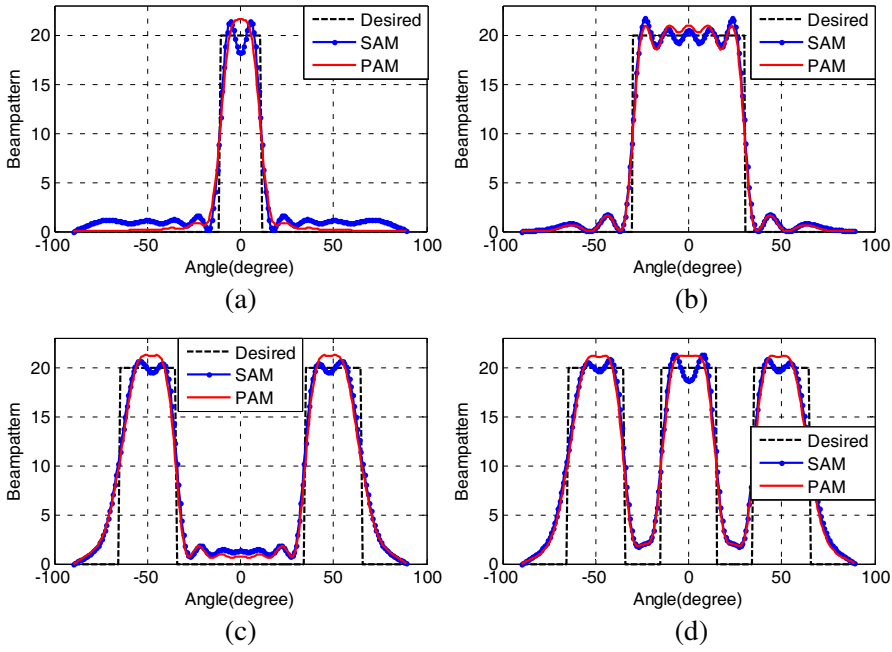

Figure 5. Beampattern matching design with four cases (a), (b), (c), (d).

Table 2. Quality parameters of the design results.

		Case 1	Case 2	Case 3	Case 4
MSE	SA	3.45	3.30	10.86	14.65
	PA	3.71	3.41	11.17	15.05
ISL	SA	−3.73 dB	−10.72 dB	−6.10 dB	−7.41 dB
	PA	−6.79 dB	−11.45 dB	−6.63 dB	−7.86 dB

the quality parameters of the designed beampatterns, see Table 2, it can be found that PAM has a lower ISL but a litter higher MSE, which is consistent with the theoretical expectation because the SAM synthesizes the beampatterns by minimizing the MSE directly and has the optimal minimum MSE. Therefore, we can conclude that though our method can not achieve the minimum MSE, it can achieve the minimum ISL and have smoother main lobes.

5. CONCLUSION

In this paper, we have studied transmit beampattern synthesis for MIMO radar with uniform elemental power. Based on the reformulation of transmit beampattern in the radian-space, we propose a MSBD method and a BMD method for beamparrern synthesis. The MSBD method consider both PSL and ISL to synthesize beampatterns and the BMD method matches beampatterns from the perspective of power approximation by minimizing ISL. We formulate both of the two design methods as convex optimization problems to obtain the optimal solutions. Finally, numerical simulations are conducted to validate our methods. It is noteworthy that our method for MSBD can be applied to beampattern synthesis with arbitrary HPBW among 0°–180° and our method for BMD can match well with the desired beampattern and have minimum ISL and smooth main lobes.

ACKNOWLEDGMENT

The authors would like to thank Dr. Jianshu Chen of the Department of Electrical Engineering, University of California, Los Angeles (UCLA), for his useful suggestions in revising this paper. The authors also like to thank the editors and the anonymous reviewers for their valuable suggestions to improve this paper.

REFERENCES

1. Li, J., Y. Xie, P. Stoica, X. Zheng, and J. Ward, "Beampattern synthesis via a matrix approach for signal power estimation," *IEEE Trans. Signal Process.*, Vol. 55, No. 12, 5643–5657, Dec. 2007.
2. Qu, Y., G. Liao, S.-Q. Zhu, and X.-Y. Liu, "Pattern synthesis of planar antenna array via convex optimization for airborne forward looking radar," *Progress In Electromagnetics Research*, Vol. 84, 1–10, 2008.
3. Hu, L., H. Liu, S. Zhou, and S. Wu, "Convex optimization applied to transmit beampattern synthesis and signal waveform design for MIMO radar," *2009 IET International Radar Conference*, 1–5, Apr. 2009.
4. Nai, S. E., W. Ser, Z.-L. Yu, and H. Chen, "Beampattern synthesis for linear and planar arrays with antenna selection by convex optimization," *IEEE Trans. Antennas Propag.*, Vol. 58, No. 12, 3923–3930, Dec. 2010.

5. Zhang, T. and W. Ser, "Robust beampattern synthesis for antenna arrays with mutual coupling effect," *IEEE Trans. Antennas Propag.*, Vol. 59, No. 8, 2889–2895, Feb. 2011.
6. Fuchs, B., "Synthesis of sparse arrays with focused or shaped beampattern via sequential convex optimizations," *IEEE Trans. Antennas Propag.*, Vol. 60, No. 7, 3499–3503, Jul. 2012.
7. Fuhrmann, D. and G. San Antonio, "Transmit beamforming for MIMO radar systems using partial signal correlation," *Proc. 38th Asilomar Conf. Signals, Syst. Comput.*, Vol. 1, 295–299, Nov. 2004,
8. Li, J. and P. Stoica, "MIMO radar with colocated antennas," *IEEE Signal. Process. Mag.*, Vol. 24, No. 5, 106–114, Sep. 2007.
9. Qu, Y., G. Liao, S.-Q. Zhu, X.-Y. Liu, and H. Jiang, "Performance analysis of beamforming for MIMO radar," *Progress In Electromagnetics Research*, Vol. 84, 123–134, 2008.
10. Roberts, W., L. Xu, J. Li, and P. Stoica, "Sparse antenna array design for MIMO active sensing applications," *IEEE Trans. Antennas Propag.*, Vol. 59, No. 3, 846–858, Mar. 2011.
11. Chen, H., X. Li, and Z. Zhuang, "Antenna geometry conditions for MIMO radar with uncoupled direction estimation," *IEEE Trans. Antennas Propag.*, Vol. 60, No. 7, 3455–3465, Jul. 2012.
12. Aittomaki, T. and V. Koivunen, "Signal covariance matrix optimization for transmit beamforming in MIMO radars," *Proc. 41th Asilomar Conf. Signals, Syst. Comput.*, 182–186, Nov. 2007.
13. Li, J., P. Stoica, and Y. Xie, "On probing signal design for MIMO radar," *Proc. 40th Asilomar Conf. Signals, Syst. Comput.*, 31–35, Pacific Grove, CA, Oct. 2006.
14. Stoica, P., J. Li, and Y. Xie, "On probing signal design for MIMO radar," *IEEE Trans. Signal Process.*, Vol. 55, No. 8, 4151–4161, Aug. 2007.
15. Aittomaki, T. and V. Koivunen, "Low-complexity method for transmit beamforming in MIMO radars," *Proc. IEEE Int. Conf. Acoust., Speech and Signal Processing (ICASSP)*, 305–308, Apr. 2007.
16. Fuhrmann, D. and G. San Antonio, "Transmit beamforming for MIMO radar systems using signal cross-correlation," *IEEE Trans. Aerosp. Electron. Syst.*, Vol. 44, No. 1, 171–186, Jan. 2008.
17. Stoica, P., J. Li, and X. Zhu, "Waveform synthesis for diversity-based transmit beampattern design," *IEEE Trans. Signal Process.*, Vol. 56, No. 6, 2593–2598, Jun. 2008.

18. Aittomaki, T. and V. Koivunen, "Beampattern optimization by minimization of quartic polynomial," *Proc. 15 IEEE/SP Statist. Signal Process. Workshop*, 437–440, Cardiff, UK, Sep. 2009.
19. Ahmed, S., J. Thompson, Y. Petillot, and B. Mulgrew, "Unconstrained synthesis of covariance matrix for MIMO radar transmit beampattern," *IEEE Trans. Signal Process.*, Vol. 59, No. 8, 3837–3849, Aug. 2011.
20. Martinezl, A. and J. Marchand, "SAR image quality assessment," *Revista de Teledeteccion*, Vol. 2, 12–18, Nov. 1993.
21. Liu, Y., Y.-K. Deng, R. Wang, and X. Jia, "Bistatic FMCW SAR raw signal simulator for extended scenes," *Progress In Electromagnetics Research*, Vol. 128, 479–502, 2012.
22. Boyd, S. and L. Vandenberghe, *Convex Optimization*, Cambridge University Press, Cambridge, UK, 2004.